



Article

Uncovering the Early Events Associated with Oligomeric A β -Induced Src Activation

Sandra I. Mota^{1,2,3} , Lígia Fão^{1,2} , Patrícia Coelho^{1,2} and A. Cristina Rego^{1,2,4,*}

¹ CNC-UC-Center for Neuroscience and Cell Biology, University of Coimbra, 3004-504 Coimbra, Portugal; sandra.mota@cnc.uc.pt (S.I.M.); ligia.fao@cnc.uc.pt (L.F.); prcoelho@cnc.uc.pt (P.C.)

² CIBB-Center for Innovative Biomedicine and Biotechnology, University of Coimbra, 3004-504 Coimbra, Portugal

³ IIIUC-Institute of Interdisciplinary Research, University of Coimbra, 3030-789 Coimbra, Portugal

⁴ Institute of Biochemistry, Faculty of Medicine, University of Coimbra, 3000-354 Coimbra, Portugal

* Correspondence: arego@fmed.uc.pt or acrego@cnc.uc.pt; Tel.: +351-239-820190 or +351-239-480038

Abstract: Soluble A β_{1-42} oligomers (A β O) are formed in the early stages of Alzheimer's disease (AD) and were previously shown to trigger enhanced Ca²⁺ levels and mitochondrial dysfunction via the activation of *N*-methyl-D-aspartate receptors (NMDAR). Src kinase is a ubiquitous redox-sensitive non-receptor tyrosine kinase involved in the regulation of several cellular processes, which was demonstrated to have a reciprocal interaction towards NMDAR activation. However, little is known about the early-stage mechanisms associated with A β O-induced neurodysfunction involving Src. Thus, in this work, we analysed the influence of brief exposure to oligomeric A β_{1-42} on Src activation and related mechanisms involving mitochondria and redox changes in mature primary rat hippocampal neurons. Data show that brief exposure to A β O induce H₂O₂-dependent Src activation involving different cellular events, including NMDAR activation and mediated intracellular Ca²⁺ rise, enhanced cytosolic and subsequent mitochondrial H₂O₂ levels, accompanied by mild mitochondrial fragmentation. Interestingly, these effects were prevented by Src inhibition, suggesting a feedforward modulation. The current study supports a relevant role for Src kinase activation in promoting the loss of postsynaptic glutamatergic synapse homeostasis involving cytosolic and mitochondrial ROS generation after brief exposure to A β O. Therefore, restoring Src activity can constitute a protective strategy for mitochondria and related hippocampal glutamatergic synapses.

Keywords: Alzheimer's disease; Src tyrosine kinase; NMDA receptor; mitochondrial dysfunction; mitochondrial morphology



Citation: Mota, S.I.; Fão, L.; Coelho, P.; Rego, A.C. Uncovering the Early Events Associated with Oligomeric A β -Induced Src Activation. *Antioxidants* **2023**, *12*, 1770. <https://doi.org/10.3390/antiox12091770>

Academic Editors: Mariano Stornaiuolo and Giuseppe Annunziata

Received: 23 August 2023
Revised: 9 September 2023
Accepted: 12 September 2023
Published: 16 September 2023



Copyright: © 2023 by the authors. Licensee MDPI, Basel, Switzerland. This article is an open access article distributed under the terms and conditions of the Creative Commons Attribution (CC BY) license (<https://creativecommons.org/licenses/by/4.0/>).

1. Introduction

Alzheimer's disease (AD) stands as the most prevalent neurodegenerative condition and a primary cause of dementia among the elderly population. It is characterised by the accumulation of extracellular senile plaques formed by amyloid-beta peptide (A β) and intracellular neurofibrillary tangles composed of hyperphosphorylated Tau [1]. AD is thought to stem from numerous early pathological processes that emerge decades before the onset of symptoms, ultimately leading to the loss of synaptic plasticity and cellular demise [2]. Synaptic function largely depends on the actin cytoskeleton and high levels of ATP [3]. In this perspective, mitochondria are the neuron's most efficient way of producing energy, also participating in Ca²⁺ storage and signaling, reactive oxygen species (ROS) production and control of apoptotic pathways [4,5]. Mitochondrial dysfunction has emerged as a key early event in AD pathogenesis triggered by A β oligomers (A β O) through both direct and indirect pathways. Indeed, soluble A β_{1-42} were shown to trigger mitochondrial Ca²⁺ rise and depolarization of the mitochondrial membrane via activation of *N*-methyl-D-aspartate receptors (NMDAR), contributing to neuronal dysfunction [6]. Furthermore, within mitochondria, A β interacts with various proteins, such as the voltage-dependent

anion-selective channel 1 (VDAC1) [7], dynamin-related protein 1 (Drp1) [8] or cytochrome C oxidase subunit 1 [9]. These interactions disrupt mitochondrial dynamics and function, ultimately leading to synaptic and neuronal damage and, consequently, cognitive decline in AD patients.

Src family kinase (SFK) is a family of non-receptor tyrosine kinases involved in several cellular processes, namely cell differentiation, signal transduction and cellular metabolism [10–12], as well as synaptic plasticity through the modulation of NMDARs [13]. SFKs are redox-sensitive and can be directly or indirectly activated by hydrogen peroxide (H_2O_2) [14]. Src is a ubiquitously expressed member of SFK [15,16] involved in several cellular processes and is activated by ROS [14]. Importantly, Src regulates neuronal plasticity and behavior through the phosphorylation of the GluN2B subunit of NMDARs at Tyr1472, increasing NMDAR's targeting of the synaptic membrane [17]. If, on the one hand, Src induces NMDARs activity, on the other hand, prolonged NMDAR activation further promotes Src activity. Importantly, Src was also identified in the intermembrane space of highly purified rat brain mitochondria [18]. In mitochondria, Src can modulate brain mitochondrial respiration [19], linking ROS signaling with mitochondrial function.

In previous studies, we demonstrated that $A\beta O$ directly interact with NMDAR subunits [20] evoking a transient increase in intracellular Ca^{2+} (Ca^{2+}_i) [21]. Sustained activation of NMDARs and $A\beta O$ massively increase Ca^{2+}_i , which is rapidly taken up by mitochondria [6], increasing ROS generation [22]. Importantly, we previously observed a decrease in Src activation/phosphorylation in the hippocampus of 3-month-old 3xTg-AD male mice but enhanced Src activation in the hippocampus of 15-month-old 3xTg-AD female mice, both occurring concomitantly with similar changes in phosphorylation of the GluN2B subunit at Tyr1472 [23]. Thus, evidence suggests that $A\beta$ -induced synaptic dysfunction is dependent on NMDARs and occurs via aberrant redox events, potentially modifying redox-sensitive proteins, such as Src. However, little is known of whether early $A\beta O$ -induced hippocampal neurodysfunction and dendritic impoverishment are linked to altered Src activation. Thus, we evaluated the influence of brief exposure to $A\beta O$ on the activation of Src kinase and further determined the role of NMDAR activation, redox changes and mitochondria on Src changes in mature primary rat hippocampal neurons. Our results show that a short incubation with $A\beta O$ evoke ROS-dependent Src activation involving NMDARs and resulting increase in Ca^{2+}_i , as well as unbalanced cytosolic and mitochondrial H_2O_2 levels and mild mitochondrial fragmentation. Our study supports an important role for Src kinase in early $A\beta O$ exposure as a process contributing to continuous glutamatergic postsynaptic dysfunction and mitochondrial changes in AD.

2. Materials and Methods

2.1. Materials

Neurobasal medium, gentamicin, B27 supplement, fetal bovine serum (FBS) and all antibiotics were purchased from GIBCO (Paisley, UK). The synthetic $A\beta_{1-42}$ and $A\beta_{42-1}$ peptide was obtained from Bachem (Bubendorf, Switzerland). Protease cocktail inhibitors, Fura-2/AM, Amplex[®] Red were purchased from Invitrogen/Molecular Probes (Life Technologies Corporation, Carlsbad, CA, USA). The compound MK-801 [(+)-5-methyl-10,11-dihydro-5H-dibenzo[a,d] cyclohepten-5,10-imine maleate] was obtained from Calbiochem (Merck Millipore, Darmstadt, Germany). Bradford protein assay was purchased from BioRad Laboratories, Inc. (Munich, Germany). TMRM⁺ probe (tetramethylrhodamine methyl ester), acrylamide, methanol, acetic acid and secondary antibodies used in Western blotting were purchased from Thermo Fisher Scientific (Rockford, IL, USA). BSA used in Western blotting was purchased from Santa Cruz Biotechnology (Santa Cruz Biotechnology, Inc., Dallas, TX, USA). ECF substrate and Western Blot PVDF membrane were purchased from GE Healthcare (Chicago, IL, USA). Trypsin, trypsin inhibitor, fatty acid free bovine serum albumin (BSA), Modified Eagle's Medium (MEM) culture medium (M0268), Dulbecco's Modified Eagle's Medium (DMEM) culture medium (D5030), SU6656, L-Glutathione ethyl ester (GSH-EE), N-acetyl-L-cysteine (NAC), hydrogen peroxide (H_2O_2),

5-fluoro-2'-deoxyuridine (5-FDU), horseradish peroxidase, MitoPY1, anti- β -actin antibody (A5316) and other analytical grade reagents were purchased from Sigma Chemical and Co. (St. Louis, MO, USA). Antibodies against Nrf2 (ab31163-500) and Phospho-Nrf2 (S40) (ab76026) were from Abcam (Cambridge, UK). Antibodies against Src (#2110) and Phospho-Src (Tyr 416) (#6943) were from Cell Signaling Technology (Danvers, MA, USA).

2.2. Primary Hippocampal Culture

Primary hippocampal neuron cultures were prepared, as described previously, in the presence of 5-fluoro-2'-deoxyuridine [24]. All animal experiments were carried out in accordance with the guidelines of the Institutional Animal Care and Use of Committee and the European Community directive (2010/63/EU) and protocols approved by the Faculty of Medicine, University of Coimbra (ref: ORBEA_211_2018) and the Direção Geral de Alimentação e Veterinária (DGAV, ref: 0421/000/000/2019). All efforts were made to minimise animal suffering and to reduce the number of animals used.

2.3. A β O Preparation

A β O preparation and A β_{42-1} oligomeric preparation were obtained, as previously described in [17]. Briefly, synthetic A β peptide was dissolved in cold 1,1,1,3,3,3-hexafluoro-2-propanol (HFIP) to a final concentration of 1 mM and aliquoted. The peptide-HFIP solutions were incubated at room temperature for 60 min, followed by 5–10 min incubation on ice. HFIP was first evaporated overnight in the hood at room temperature, and then the remaining was removed in a Speed Vac (Ilshin Lab. Co. Ltd., Ede, The Netherlands). Dried HFIP film was stored at -80 °C and, when necessary, resuspended to make a 5 mM solution in anhydrous dimethyl sulfoxide and then dissolved in phenol red-free Ham's F-12 medium without glutamine to a final concentration of 100 μ M and incubated overnight at 4 °C. The preparation was centrifuged at $14,000 \times g$ for 10 min at 4 °C to remove insoluble aggregates, and the supernatant containing soluble oligomers and monomers was transferred to prelubricated clean tubes (Costar) and stored at -20 °C. Protein content was determined using the BioRad protein assay and quantified using a microplate reader Spectra Max Plus 384 (Molecular Devices, San Jose, CA, USA). The presence of different assembly peptide forms (monomers, oligomers and/or fibrils) in the preparation was evaluated by 4–16% nondenaturing Tris-Tricine polyacrylamide gel electrophoresis and further staining with a solution of 0.5% Coomassie in 45% methanol and 10% acetic acid. Typically, our preparations showed only small oligomers (16 to 24 kDa) and no monomers or fibrils (data not shown).

2.4. Experimental Conditions

Mature primary hippocampal neurons (17–18 DIV) were exposed to 1 μ M of soluble A β_{1-42} oligomers (A β O) for 5, 10 or 30 min or acutely. When indicated, the reverse peptide A β_{42-1} was used to confirm the specific effect of A β O. To evaluate the role of oxidative stress in A β O-induced effects, cells were pre-exposed to antioxidants GSH (0.1 mM) and Mitotempo (MT; 1 μ M), a mitochondrial antioxidant, for 24 h and N-acetyl-L-cysteine (NAC; 1 mM), a precursor of GSH, for 1 h. The effect of Src inhibition was also assessed by using SU6656 (5 μ M) after 1 h pretreatment [18], as well as the effect of NMDARs inhibition by using MK-801 (10 μ M; 10 min pretreatment). All incubations were performed in a conditioned culture medium. For live experiments, cells were maintained in Mg²⁺-free Na⁺ medium (containing 140 mM NaCl, 5 mM KCl, 1 mM CaCl₂, 10 mM Glucose, 10 mM HEPES, pH 7.4/NaOH) supplemented with glycine (20 μ M) and serine (30 μ M).

2.5. Protein Extraction and Western Blotting

Total extract protein was obtained after washing cells 3 times in ice-cold PBS and then scraping them in RIPA extraction buffer (containing 150 mM NaCl, 50 mM Tris HCl, 5 mM EGTA, 1% Triton X-100, 0.1% SDS, 0.5% deoxycholate, pH 7.5) supplemented with 100 nM okadaic acid, 1 mM PMSF, 25 mM NaF, 1 mM Na₃VO₄, 1 mM DTT and 1 μ g/mL protease

inhibitor cocktail (chymostatin, pepstatin A, leupeptin and antipain). Homogenates were then lysed in an ultrasonic bath (UCS 300—THD; at heater power 200 W and frequency 45 kHz) for 10 sec and centrifuged for 10 min at $20,800 \times g$ (4°C) to remove cell debris, and the supernatant was collected. Protein content was determined using the Bradford protein assay. Equivalent amounts of protein samples (20 μg) were denatured at 95°C for 5 min with 6x concentrated loading buffer (containing 300 mM Tris-HCl pH 6.8, 12% SDS, 30% glycerol, 600 mM DTT, 0.06% bromophenol blue), and separated by 8–12% SDS-PAGE gel electrophoresis and electroblotted onto polyvinylidene difluoride (PVDF) membranes. Membranes were further blocked 1h at room temperature with 5% (*w/v*) BSA in Tris Buffered Saline (containing Tris-HCl 25 mM pH 7.6 and NaCl 150 mM) with 0.1% Tween-20 (TBS-T) and then incubated overnight at 4°C with primary antibodies: β Actin (1:5000), Nrf2 (1:500), Phospho-Nrf2 (S40) (1:500), Src (1:1000); Phospho-Src (Tyr 416) (1:1000). Antimouse or antirabbit IgG secondary antibody conjugated to the alkaline phosphatase (1:10,000) prepared in 1% (*w/v*) BSA in TBS-T was used for 1 h at room temperature. Immunoreactive bands were visualised by alkaline phosphatase activity after incubation with ECF reagent and visualised by using a BioRad ChemiDoc Touch Imaging System (BioRad, Hercules, CA, USA) and quantified using Image Lab analysis software (BioRad).

2.6. Intracellular Calcium Levels

Primary hippocampal neurons were incubated with a 10 μM Fura-2/AM fluorescent probe for 40 min at 37°C in a conditioned medium before pre-incubation ending. After a washing step with Na^+ medium (containing 140 mM NaCl, 5 mM KCl, 1 mM CaCl_2 , 1 mM MgCl_2 , 10 mM Glucose, 10 mM Hepes, pH 7.4/NaOH), Fura-2 fluorescence was monitored in Mg^{2+} -free Na^+ medium plus serine/glycine using a Spectrofluorometer Gemini EM (Molecular Devices, San Jose, CA, USA) microplate reader at a 340/380 nm excitation and 510 nm emission wavelengths. Fura-2 fluorescence was recorded for 2 min (basal values) and a further 5 min after stimuli with $\text{A}\beta\text{O}$. Fluorescence values (ratio 340/380) were normalised to the baseline.

2.7. Measurement of Cellular H_2O_2 Levels

H_2O_2 released by primary hippocampal neurons was determined using the extracellular Amplex[®] Red assay through the monitoring of resorufin fluorescence (excitation 550 nm; emission 580 nm), the stoichiometry product of H_2O_2 reacting with Amplex[®] Red reagent (10-acetyl-3,7-dihydroxyphenoxazine). After a washing step with Na^+ medium, H_2O_2 levels were measured in Mg^{2+} -free Na^+ medium plus serine/glycine supplemented with 10 μM Amplex[®] Red plus 0.5 units/mL of horseradish peroxidase for 3 min (basal) and for 30 min after stimuli using a microplate reader Spectrofluorometer Gemini EM (Molecular Devices, San Jose, CA, USA).

2.8. Evaluation of Mitochondrial H_2O_2 Levels

MitoPY1 was used to measure mitochondrial-derived H_2O_2 in primary hippocampal neurons. Cells were incubated with 10 μM MitoPY1 in Na^+ medium at 37°C for 30 min. Then, cells were washed to remove the not-internalised probe, and changes in mitochondrial H_2O_2 levels were analysed in Mg^{2+} -free Na^+ medium plus serine/glycine using confocal images obtained using a $20\times$ objective with NA = 0.8 on a Carl Zeiss Axio Observed Z1 inverted confocal microscope using the CSU-X1M spinning disc technology (Zeiss, Jena, Germany). Basal mitochondrial H_2O_2 levels were recorded for 15 min basal followed by 30 min after stimuli (one frame every minute). Fluorescence intensity was quantified using FIJI software (version 2.1.0/1.51w).

2.9. Mitochondrial Membrane Potential Assessment

Primary hippocampal neurons were incubated in a conditioned culture medium with the mitochondrial membrane potential (mmp)-sensitive probe (TMRM⁺ at 300 nM,

under quench mode) for 30 min in the incubator (37 °C, 5% CO₂) before the end of AβO incubation. After a washing step with Na⁺ medium, mmp was measured in cell population in Mg²⁺-free Na⁺ medium plus serine/glycine, plus TMRM⁺, using a microplate reader Spectrofluorometer Gemini EM (Molecular Devices, San Jose, CA, USA) (540 nm excitation, 590 nm emission). Changes in mmp were assessed by the analysis of TMRM⁺ fluorescence dequenching after complete mitochondrial depolarization (mmp collapse) achieved by adding a protonophore [2 μM carbonyl cyanide-4-(trifluoromethoxy)phenylhydrazone (FCCP)] plus oligomycin (2 μg/mL) to prevent ATP synthase reversal.

2.10. Cell Transfection

Primary hippocampal neurons were cotransfected with plasmids codifying for MitoDsRed (to label mitochondria) plus GFP (to fill in the cell) when still immature (at 8 DIV) using calcium phosphate coprecipitation protocol as described in [24].

2.11. Evaluation of Mitochondrial Morphology

Mitochondrial morphology was assessed as in [24]. Briefly, hippocampal neurons, cotransfected with MitoDsRed plus GFP, were washed and incubated in Na⁺ medium plus serine/glycine at 37 °C for mitochondrial movement studies. An image of neuronal projections (MitoDsRed plus GFP) was acquired using a 63× objective with NA = 1.4 on a Carl Zeiss Axio Observed Z1 inverted confocal microscope using the CSU-X1M spinning disc technology (Zeiss, Jena, Germany) after 10 min incubation with AβO in the absence or presence of SU6656 or MK-801. To assess mitochondrial morphology, the macros AutoROI and MitoProtAnalyser for FIJI were applied in the last image acquired to assess the following parameters per mitochondria: aspect ratio (major axis/minor axis) and circularity ($4\pi \times \text{area}/\text{perimeter}^2$), which reflect length and degree of fragmentation, respectively.

2.12. Statistical Analyses

Data were expressed as the mean ± SEM of the number of experiments or elements (neuritis or mitochondria) indicated in the figure legends. The normal distribution of each population was analysed, and all experimental groups were considered nonparametric. Thus, comparisons among multiple groups (relative to control or AβO treatment) were performed by nonparametric one-way analysis of variance (ANOVA) followed by the Kruskal-Wallis Multiple Comparison post hoc test. The Mann-Whitney U-test was also performed for comparison between the two populations, as described in figure legends. Significance was defined as $p < 0.05$.

3. Results

3.1. AβO Induce Src Kinase Activation Involving NMDARs Activation and Enhanced H₂O₂ Levels

The effect of brief exposure to AβO (1 μM) on the activation of the redox sensor protein, the nonreceptor Src tyrosine kinase family (Src), was first investigated in mature primary hippocampal neurons. We analysed the levels of total and phosphorylated Src at residue Tyr416, which reflects its activation [25], in hippocampal neurons treated with AβO for up to 30 min in the absence or presence of pharmacological compounds (Figure 1). The concentration of AβO was selected based on the levels of soluble Aβ₁₋₄₂ determined in pyramidal neurons derived from the AD patient's hippocampus [~3 μM [26]] and on previous results obtained in the group in both hippocampal [24] and cortical primary neurons [6,21].

Results shown in Figure 1A and Figure S3 evidence that exposure for 10 and 30 min to AβO causes an increase in the levels of phosphorylated Src (iii) and P(Tyr416)Src/Src ratio (i) while maintaining the levels of total Src (ii) when compared to the control condition (i.e., nontreated cells). Phosphorylation of Src at residue Tyr 416 reflects its activation [16], largely suggesting that a short exposure to AβO induces Src activation.

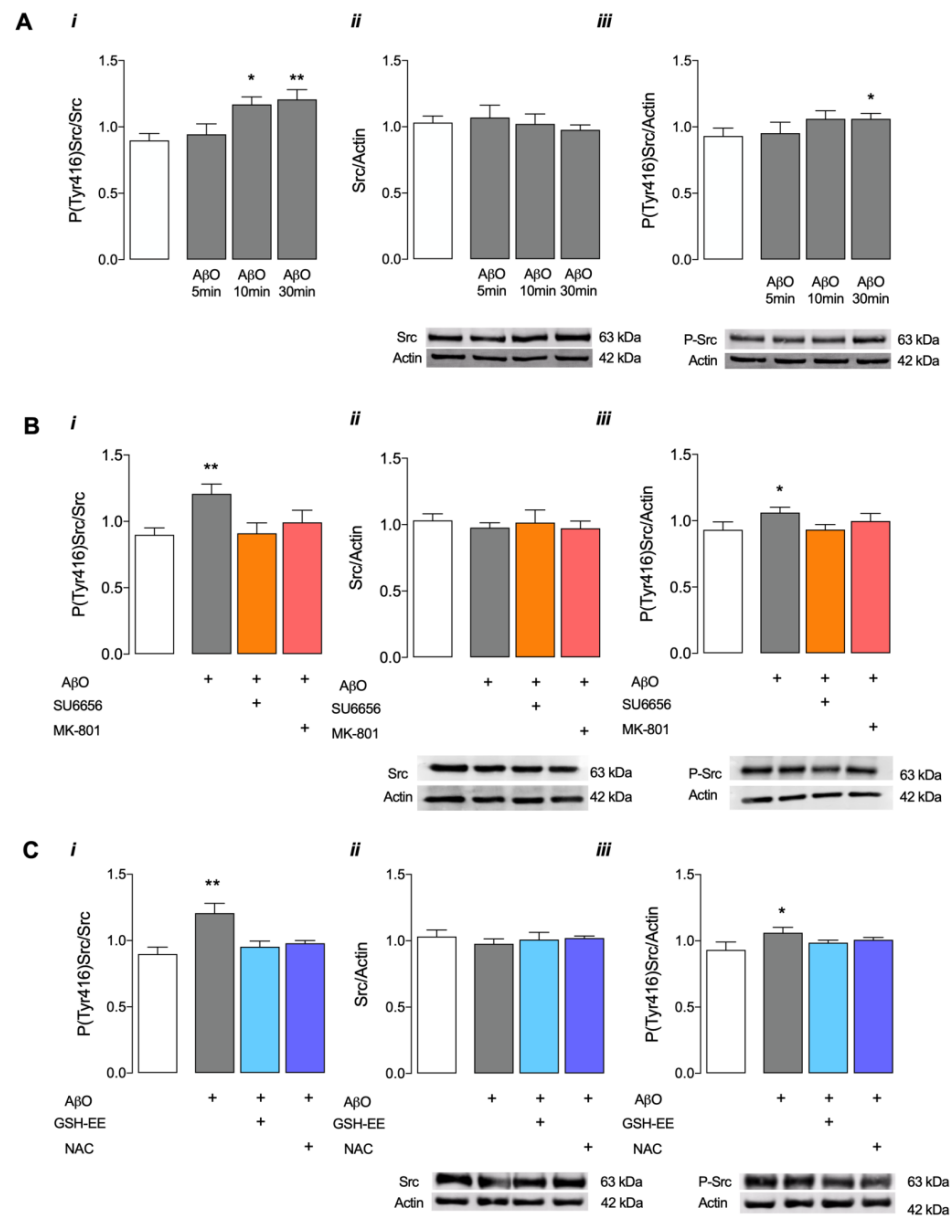


Figure 1. Src total and phosphorylated protein levels in mature hippocampal neurons after exposure to AβO. Hippocampal mature neurons (17 DIV) were incubated with 1 μM AβO for 5, 10 and 30 min in (A), and the levels of P(Tyr416)Src/Src (Ai,Bi,Ci), Src/actin (Aii,Bii,Cii) and P(Tyr416)Src/actin (Aiii,Biii,Ciii) were evaluated using Western blotting. The effects of SU6656 (5 μM) and MK-801 (10 μM) in (B), as well as NAC (1 mM) and GSH-EE (0.1 mM) in (C), were evaluated in cells exposed to AβO (1 μM), for 30 min. Data are expressed in arbitrary units as the mean ± SEM of n = 3 to 10 experiments. Statistical analysis: * p < 0.05 and ** p < 0.01 vs. control (Kruskal-Wallis followed by Dunn’s post hoc test).

To confirm that under these conditions Src activation could be modulated by NMDAR activation and ROS levels, we pre-incubated cells with MK-801 (Figure 1B) or with antioxidants (Figures 1C and S5) and determined the influence of AβO incubated for 30 min. Pretreatment with MK-801, a noncompetitive NMDAR inhibitor, prevented the phosphorylation/activation of Src induced by AβO (Figures 1B and S4), suggesting that activation of NMDARs is required for AβO-induced Src activation. Of note, pre-incubation with SU6656, an inhibitor of the SFK, similarly inhibited AβO-evoked Src activation (Figures 1B and S4). Furthermore, AβO-induced increase in P(Tyr416)Src levels was largely prevented in cells

pretreated with both antioxidants GSH-EE (a cell-permeable derivative of reduced glutathione, GSH) and NAC (a precursor of GSH synthesis by providing Cys), suggesting that the activation of Src is also modulated by oxidative events. Results obtained in Figure 1 evidence that short exposure of mature hippocampal neurons to A β O induces the phosphorylation/activation of Src kinase in a process mediated by both NMDARs and redox changes.

To further support the involvement of NMDARs on A β O-induced Src activation, we measured Ca $^{2+}$ _i levels (Figure 2) following immediate exposure to A β O in the absence or presence of MK-801, SU6656 and antioxidants. A β O (1 μ M) evoked an immediate rise in Ca $^{2+}$ _i in mature hippocampal neurons (Figure 2A,D). Of relevance, this effect was specific to the A β _{1–42} oligomeric form since the reverse peptide A β _{42–1} did not induce a significant change in Ca $^{2+}$ _i (Figure 2A,D). Figure 2B shows that prior inhibition of NMDARs using MK-801 completely prevented the entry of Ca $^{2+}$ through the receptor. Similarly, prior inhibition of Src kinases with SU6656 also prevented the rise in Ca $^{2+}$ _i in neurons exposed to A β O, probably due to the role of Src on NMDAR modulation [17]. Importantly, prior incubation of cells with antioxidants (GSH-EE; NAC; or Mitotempo, MT, a mitochondria-targeted superoxide dismutase mimetic) did not significantly change the Ca $^{2+}$ _i response in hippocampal neurons subjected to immediate A β O exposure (Figure 2C,D), suggesting that intraneuronal ROS generation and/or cellular oxidation events do not influence the increase in Ca $^{2+}$ _i.

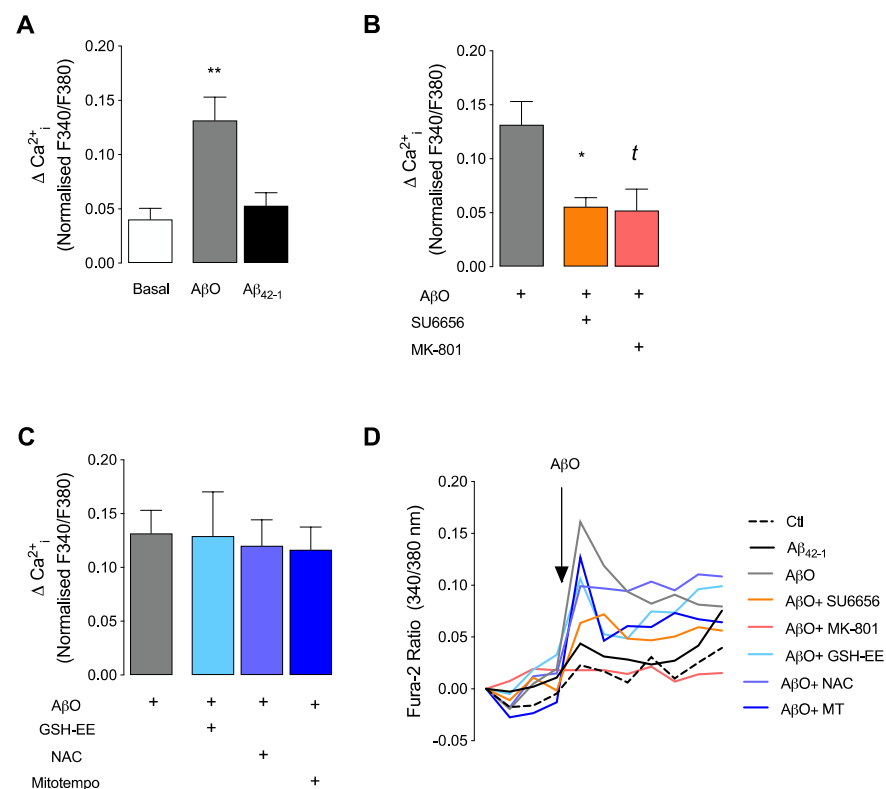


Figure 2. Intracellular Ca $^{2+}$ levels after acute treatment with A β O in mature hippocampal neurons. Basal Ca $^{2+}$ _i levels were recorded for 2 min in mature hippocampal neurons (17 DIV), and the effect of A β O (1 μ M) was recorded for a further 5 min. The effect of A β O was calculated by analysing the Fura-2 fluorescence ratio at 340/380 nm. The effect of the reverse peptide A β O_{42–1} (1 μ M) was evaluated in (A). The effects of SU6656 (5 μ M) and MK-801 (10 μ M) were analysed in (B). The influence of antioxidants GSH-EE (0.1 mM), NAC (1 mM) and Mitotempo (MT; 1 μ M) was evaluated in (C). Results were plotted as the difference between the last and the first values achieved before and after the addition of A β O. Graphic (D) is the representative line chart (normalised to baseline). Data are expressed as the mean \pm SEM of n = 3 to 10 experiments, run in triplicates. Statistical analysis: * p < 0.05 and ** p < 0.01 vs. control (Kruskal-Wallis followed by Dunn’s post hoc test), ^t p < 0.05 (Mann-Whitney).

In Figure 3, we also evaluated the levels of H₂O₂ released by hippocampal neurons following immediate A β O (1 μ M) exposure. Results evidence a significant rise in the levels of H₂O₂ released by cells right after A β O incubation; this result is specific to A β _{1–42} form, since the reverse peptide (A β _{42–1}) did not induce significant changes in H₂O₂ levels (Figure 3A). Results depicted in Figure 3B demonstrate not only that pretreatment of hippocampal neurons with antioxidants (GSH-EE, NAC or MT) prevents the increase in H₂O₂ levels induced by the peptide oligomers but also that pre-incubation with MK-801 or SU6656 prevents the effect of A β O on H₂O₂ levels. These data suggest that, under these conditions, ROS generation is dependent on both NMDAR and Src activation.

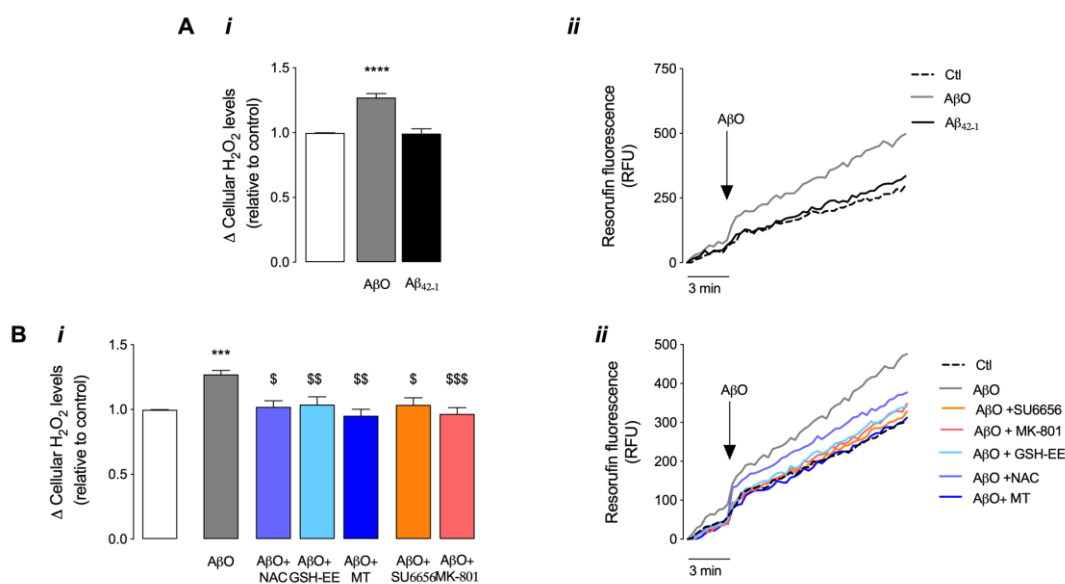


Figure 3. H₂O₂ levels following A β O stimulus in mature hippocampal neurons. Cellular H₂O₂ levels were evaluated by monitoring the fluorescence of resorufin. Basal fluorescence was recorded for 3 min, while the effect of A β O (1 μ M) was recorded for 30 min (**Aii,Bii**). The effect of the reverse peptide A β _{42–1} (1 μ M) was evaluated in (**Ai,ii**). The influence of NAC (1 mM), GSH-EE (0.1 mM) and Mitotempo (1 μ M) or the effect of SU6656 (5 μ M) and MK-801 (10 μ M) were evaluated in (**Bi,ii**) in neurons exposed to A β O. In graphics (i), results were plotted as the difference between the last value achieved and the basal value before A β O addition, relative to the control. Graphics (ii) are the representative line charts (normalised to baseline). Data are expressed as the mean \pm SEM of n = 3 to 10 experiments, run in quadruplicates. Statistical analysis: *** $p < 0.001$ or **** $p < 0.0001$ vs. control, \$ $p < 0.05$, \$\$ $p < 0.01$ and \$\$\$ $p < 0.001$ vs. A β O (Kruskal-Wallis followed by Dunn’s post hoc test).

Phosphorylation of the transcription factor Nrf2 (nuclear factor erythroid 2-related factor 2) at Ser40 is a signal for its nuclear translocation and an indicator of its activation following increased levels of cellular ROS [27]. Concordantly with A β O-immediate rise in H₂O₂ (data shown in Figures S1, S6 and S7) evidence a significant increase in the phosphorylation of Nrf2 at Ser40, starting as early as 5 min after A β O exposure, while extracellular H₂O₂ exposure was used as a positive control.

These data show that A β O-induced Src activation is the result of a signaling pathway apparently initiated by the activation of NMDARs with the concomitant rise in Ca²⁺_i, leading to enhanced H₂O₂ levels, which further evokes Src activation/phosphorylation. The observation of a time-dependent (5–30 min) decrease in P(Ser40)Nrf2/Nrf2 (Figures S1, S6 and S7) and an increase in P(Tyr416)Src/Src (Figure 1A) largely suggests that A β O-induced ROS generation linked to Nrf2 activation precedes Src activation in hippocampal neurons. Importantly, a feed-forward modulation of Src on both Ca²⁺_i and H₂O₂ levels induced by A β O cannot be excluded; data suggest that initial activation of Src after A β O exposure can evoke a continuous activation of NMDARs and a potential long-term amplification of A β O-induced effects in hippocampal neurons.

3.2. A β O-Induced Src Activation Regulates Mitochondrial H₂O₂ and Mild Mitochondrial Fragmentation

A β directly targets mitochondria [28,29], which also produce ROS, leading to the accumulation of ROS and subsequent oxidative unbalance. Of relevance, Src was found in mitochondria, where it can regulate cell survival by phosphorylating respiratory chain components [19], linking ROS signaling with mitochondrial function. Since A β O exposure leads to an increase in H₂O₂ in hippocampal neurons (Figure 3), we further investigated the impact of short exposure to A β O on mitochondrial H₂O₂ production and changes in mmp and the possible role of Src kinase (Figure S2).

Results depicted in Figure 4A,B show that 1 μ M A β O induces a significant increase in the levels of mitochondrial H₂O₂. Interestingly, this increase occurs after a delay of about 15 min (Figure 4Aiii,Biii), in contrast with the immediate changes in H₂O₂ cellular release observed in Figure 3, the latter probably resulting from an immediate A β O-evoked H₂O₂ production in the cytosol, prone to influence Nrf2 activation (Figure S1). As expected, both cellular and mitochondrial-selective antioxidants, namely NAC and MT, prevent the increase in overall mitochondrial H₂O₂ levels induced by the A β O stimulus (Figure 4Ai,iii,iv). Furthermore, inhibition of NMDARs or Src also prevents A β O-induced mitochondrial H₂O₂ production (Figure 4Bi,iii,iv); in this perspective, a direct effect of SU6656 on mitochondrial Src and its impact on mitochondrial H₂O₂ production cannot be excluded. Importantly, analysis of mitochondrial H₂O₂ specifically within neurites evidences similar results, although only MT is able to totally prevent the increase in mitochondrial H₂O₂ production induced by A β O stimulus (Figure 4Aii), while NAC (Figure 4Aii), MK-801 or SU6656 (Figure 4Bii) only partially prevent the effect mediated by the peptide oligomers.

We further assessed if short exposure to A β O (1 μ M) for 10 min (Figure S2A) or 30 min (Figure S2B) induces changes in mmp. Results shown in Figure S2 evidence no significant changes in mmp induced by short exposure to A β O, which is not influenced by MK-801 or SU6656 either.

Data indicate that mitochondrial H₂O₂ production is not an initial neuronal event after exposure to A β O, although it is largely influenced by NMDAR and Src activation and occurs without evidence of mitochondrial depolarization.

To deepen the impact of short A β O exposure and the role of Src on mitochondria, we further evaluated dynamic changes in mitochondrial morphology in mature hippocampal neurites (Figure 5). Figure 5A shows a representative mitochondrial mask obtained with the MitoProtAnalyser macro for Fiji that is further used by the macro to evaluate the mitochondrial aspect ratio (Figure 5B) and circularity (Figure 5C). Exposure to A β O for 10 min induces a slight but significant decrease in mitochondrial aspect ratio, which is prevented by pretreatment with SU6656 (Figure 5B). Importantly, the effect of A β O on mitochondrial aspect ratio occurs concomitantly with a slight but significant increase in mitochondrial circularity (Figure 5C), prevented both by SU6656 and MK-801. These results evidence that A β O short exposure induces mild mitochondrial fragmentation dependent on Src activation.

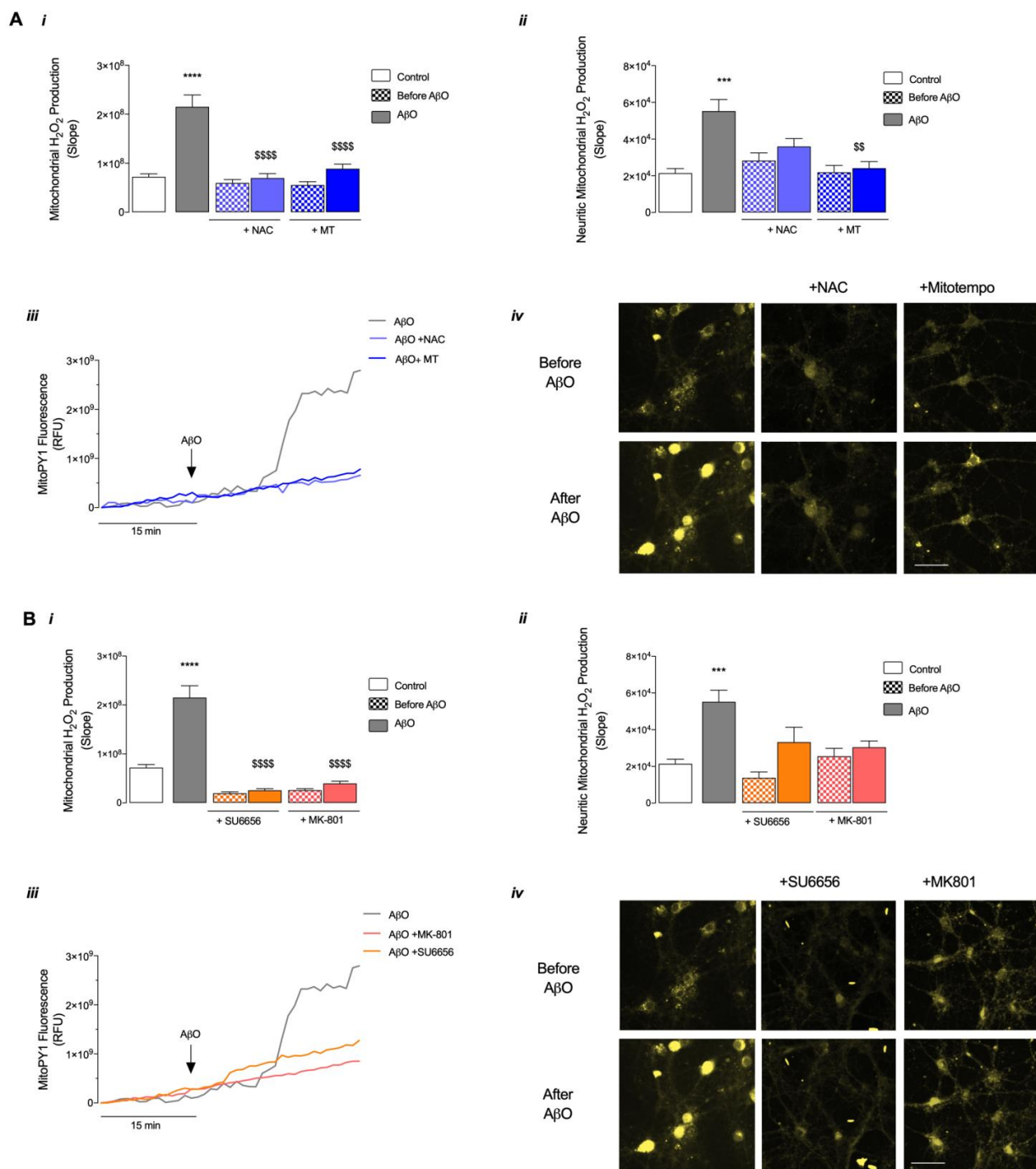


Figure 4. Mitochondrial H₂O₂ levels following AβO exposure in mature hippocampal neurons. **(A,B)** The levels of mitochondrial H₂O₂ were evaluated by monitoring the fluorescence of MitoPY1 (10 μM) in mature hippocampal neurons (17 DIV). Basal mitochondrial H₂O₂ was recorded for 15 min, and the effect of AβO (1 μM) was recorded for 30 min. The effects of Mitotempo (MT, 1 μM) and NAC (1 mM) **(A)** or SU6656 (5 μM) and MK-801 (10 μM) **(B)** were also evaluated. In graphics *(i)*, the slope was calculated using values of RFU before and after AβO addition. Graphics *(ii)* slope was calculated by assessing fluorescence within neurites, only using values of RFU before and after AβO addition. *(iii)* Representative line charts (normalised to baseline). *(iv)* Fluorescence image of representative cells before and after the treatment. Scale bar: 50 μm. Data are the mean ± SEM of 20 to 100 single-cell analyses obtained from 2 to 5 independent experiments. Statistical analysis: *** *p* < 0.001 or **** *p* < 0.0001 vs. control/“no treatment” (Kruskal-Wallis followed by Dunn’s post hoc test); \$\$ *p* < 0.01 or \$\$\$\$ *p* < 0.0001 vs. AβO (Kruskal-Wallis followed by Dunn’s post hoc test).

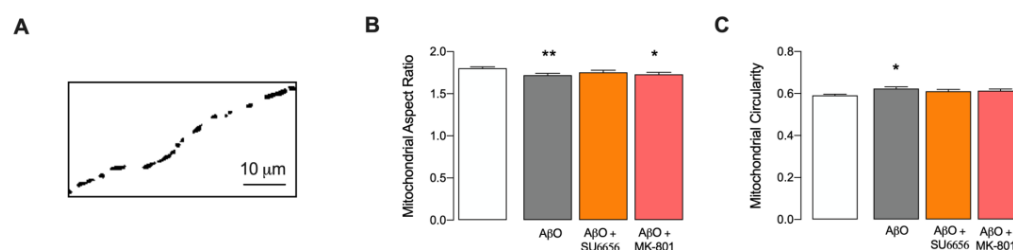


Figure 5. Dendritic mitochondrial morphology following A β O stimulus in mature hippocampal neurons. Cells cotransfected with pDsRed2-Mito and GFP plasmids were treated with A β O for 10 min, and mitochondrial morphology was measured using a 63 \times objective, NA = 1.4 on a spinning disk equipped Zeiss LSM 710 inverted microscope. The effect of SU6656 (5 μ M) and MK-801 (10 μ M) were also evaluated. (A) shows a representative mask of mitochondria obtained using the MitoProt-Analyser macro in Fiji used to assess mitochondrial morphology parameters, namely (B) aspect ratio and (C) circularity. Data are expressed as the mean \pm SEM of $n = 6$ –10 independent experiments, considering an average of 9 neuritis per analysis. Statistical analysis: * $p < 0.05$, ** $p < 0.01$ vs. Control (Kruskal-Wallis followed by Dunn's post hoc test).

4. Discussion

AD is characterised by synaptic dysfunction and neuronal loss. The role of soluble species of A β in triggering neuronal dysfunction before cell death is largely accepted [30]. In previous studies, we demonstrated that A β O directly interact with NMDAR subunits (GluN1 and GluN2B) [20] evoking a transient increase in Ca $^{2+}$ _i [21]. A β O and agonist-selective NMDAR activation concur in increasing Ca $^{2+}$ _i, which is rapidly and directly taken up by mitochondria and through the endoplasmic reticulum [6]. Excessive ROS production under these conditions [22] may then activate several redox-sensitive proteins, including Src kinase [14]. Indeed, our findings provide evidence that short exposure to A β O triggers the activation of Src through H $_2$ O $_2$ -dependent mechanisms, primarily involving the activation of NMDARs. This activation leads to an excessive buildup of Ca $^{2+}$ _i, resulting in an imbalance of cytosolic and mitochondrial H $_2$ O $_2$ levels. Interestingly, despite inducing mild mitochondrial fragmentation, brief A β O exposure per se does not cause significant persistent changes in mmp, a translation of its function.

Previous studies demonstrated that incubation of human and rat brain cortical cultures with aggregated A β_{25-35} induced a very rapid (about 1 min) and marked increase in Tyr phosphorylation of numerous neuronal proteins, including focal adhesion kinase (FAK). This effect was blocked by the addition of the SFK inhibitor 4-amino-5-(4-chlorophenyl)-7(t-butyl)pyrazol(3,4-d)pyrimidine (PP2) [31], suggesting that A β_{25-35} induced an almost immediate activation of SFKs. Conversely, intracerebroventricular injection of A β O in mice or 60 min incubation of hippocampal slices with A β O decreased Src phosphorylation [32]. Interestingly, we previously showed a decrease in Src phosphorylation/activation in the hippocampus and cortex of a 3-month-old 3xTg-AD mouse male, while an increase in Src phosphorylation was observed in the hippocampus of a 15-month-old 3xTg-AD mouse female [23], suggesting a dynamic regulation of this SFK. Herein, we observed a significant increase in the levels of phosphorylated Src after brief exposure (10, 30 min) to A β O, indicating that short exposure to A β O causes Src activation, while chronic exposure can be dynamically modulated so that a decrease in its activity might constitute a defense mechanism to avoid overstimulation of pathologically Src-dependent pathways. These differences may also be the result of the influence of other cell types; however, in primary hippocampal neurons cultured in the presence of a mitotic inhibitor, as ours, these are relatively absent and thus are not expected to contribute to modulate Src phosphorylation.

In a model of chronic pain using inferior alveolar nerve transection (IANX), the authors observed the colocalization of Src and GluN1, an NMDAR subunit [33]. Interestingly, in this model, the administration of memantine (an antagonist of NMDAR) decreased IANX-induced upregulation of phosphorylated Src, while PP2 had no effect on GluN1 protein levels [33], suggesting a prior and required activation of NMDAR for Src activation.

In an adult rat, the intracerebroventricular injection with A β _{25–35} induced Src-dependent Tyr phosphorylation of PSD-95 after the activation of GluN2A- and GluN2B-containing NMDARs [34]. In this study, we were able to decipher a sequence of cellular events, culminating in Src activation dependent on A β O-induced NMDAR activation, as demonstrated by the effect of MK-801. A β O-mediated initial NMDAR activation and Ca²⁺_i rise were associated with increased cytosolic H₂O₂ levels linked to Nrf2 phosphorylation/activation and a subsequent increase in mitochondrial H₂O₂ levels. Interestingly, in levodopa-induced dyskinesia, Src S-nitrosylation was caused by a neuronal nitric oxide synthase (nNOS)/NO signal activated by Ca²⁺ influx via GluN2B-containing NMDAR, which subsequently facilitated Src autophosphorylation (at Tyr416) and further phosphorylated GluN2B, demonstrating a positive feed-forward effect leading to GluN2B Tyr phosphorylation [35]. Our data is in agreement with a vicious cycle in which NMDAR-dependent Src activation/phosphorylation further promotes NMDAR activation.

Oxidative stress is one of the main processes involved in AD pathogenesis [36]. In former studies, Behl and colleagues demonstrated that A β (25–35 and 1–40 peptides) caused increased H₂O₂ levels and accumulation of lipid peroxides in primary cortical neurons, B12 and PC12 cells, affecting cell metabolism and survival [37]. Similar results were observed in A β -treated N2a neuroblastoma cells [38,39] and APP/PS1 transgenic cell lines associated with elevated A β levels, leading to cell death [38]. Herein, we evidence that acute A β O stimulus of mature hippocampal neurons is accompanied by an immediate increase in H₂O₂ released by cells and a delayed increase in mitochondrial H₂O₂ levels. Our data also show that the elevation of H₂O₂ levels is apparently the result of previous Ca²⁺_i dyshomeostasis, in accordance with previous findings [40]. Interestingly, we observe a primer role of non-mitochondrial/cytosolic H₂O₂ coincident with enhanced phosphorylation/activation of Nrf2 and subsequent P-Src and increased mitochondrial H₂O₂. In agreement, extracellular H₂O₂ targets mitochondria and induces increased mitochondrial ROS in SH-SY5Y human neuroblastoma cells [41]. Of note, Src was previously detected in mitochondria [18,42]. Moreover, we previously demonstrated that restoring active SFK levels improves mitochondrial morphology and function in a cellular model of Huntington's disease [42]. These data suggest that changes in Src activation following short exposure to A β O might also occur within mitochondria. Since Src is involved in the modulation of brain mitochondrial respiration through the phosphorylation of complexes I, III and IV [19], changes in mitochondrial Src activation could reflect on mitochondrial function and thus potentiate the initial toxic effects of A β O. Nevertheless, no major changes in mmp were observed, which might be accounted for by a less sensitive fluorescence analysis of the overall cell population.

Several reports support mitochondrial dysfunction as an early event in AD etiology [43] and implicate A β in AD-associated mitochondrial dysfunction [44]. Apart from their important metabolic role, mitochondrial dynamic changes in morphology are also affected in AD. Exposure of A β to HT22 immortalised mouse primary hippocampal cells increased mitochondrial density and reduced mitochondrial length [45], suggesting mitochondrial fragmentation. Similarly, treatment of Wistar rats with A β _{1–42} induced a decrease in the levels of mitofusin-2 protein and translocation of Drp-1 to mitochondria [46], correlating with increased mitochondrial fragmentation. Primary hippocampal and cortical neurons from Tg2576 mice evidenced increased mitochondrial fission, decreased fusion and abnormal mitochondrial function [47]. Moreover, we previously demonstrated that prolonged A β O (1 μ M, for up to 24 h) treatment caused mitochondrial fragmentation in mature primary hippocampal neurons [24] or in HT22 hippocampal cells without evidence of cell death [48]. Here, we evidence that short exposure to the same concentration of A β O is enough to induce a mild decrease in mitochondrial aspect ratio and an increase in mitochondrial circularity, supporting some degree of mitochondrial fragmentation. Importantly, these effects were completely prevented by the Src inhibitor SU6656 and only partially by the NMDARs antagonist MK-801, suggesting a possible role of specific mitochondrial Src on the modulation of A β O-induced mitochondrial morphology.

5. Conclusions

We demonstrate, for the first time, that brief exposure to A β O induces H₂O₂-dependent Src activation. Moreover, we evaluated potential sequential cellular events culminating in Src activation: (i) NMDARs activation linked to increased Ca²⁺_i; (ii) cytosolic H₂O₂ levels unbalance and Nrf2 activation; and (iii) enhanced mitochondrial H₂O₂ levels and mild organelle fragmentation, associated with Src phosphorylation, anticipating its role in this organelle.

In the past 10 years, interest in SFK targeting for the treatment of AD has increased. Fyn, an Src homolog, was the first to attract attention due to its interaction with both A β and Tau, as well as NMDARs [49]. This interest led to a phase Ib clinical trial (NCT01864655) to assess the safety, tolerability, and central nervous system availability of AZD0530 (saracatinib), an inhibitor of Src and Abl family kinases1 with a high potency for Src and Fyn in mild to moderate AD patients [50]. In the same year, AZD0530 was shown to rescue spatial memory deficits, synaptic depletion, Tau phosphorylation and deposition, and reduce microglial activation in APP/PS1 mice [51]. These were followed by a phase 2a randomised clinical trial (NCT02167256) to assess the effect of AZD0530 on cerebral metabolic decline in mild AD patients [52]. Unfortunately, there were no statistically significant effects of AZD0530 treatment on the cerebral metabolic rate for glucose, cognitive functions and total brain or ventricular volume, and patients exhibited several adverse events; however, it showed a trend for slowing down the reduction in hippocampal volume and entorhinal thickness [52]. Based on these results and our data, novel compounds ought to be produced to improve their selectivity towards specific SFK members, which could be tested in earlier stages of AD aiming to prevent major changes in mitochondria and hippocampal glutamatergic synapses.

Supplementary Materials: The following supporting information can be downloaded at <https://www.mdpi.com/article/10.3390/antiox12091770/s1>, Figure S1: Nrf2 total and phosphorylated protein levels in mature hippocampal neurons after A β O exposure; Figure S2: Mitochondrial membrane potential following A β O exposure in mature hippocampal neurons; Figure S3: Entire Western blot membranes which correspond to the cropped Western blot band shown in Figure 1Aii and 1Aiii; Figure S4: Entire Western blot membranes which correspond to the cropped Western blot band shown in Figure 1Bii and 1Biii; Figure S5: Entire Western blot membranes which correspond to the cropped Western blot band shown in Figure 1Cii and 1Ciii; Figure S6: Entire Western blot membranes which correspond to the cropped Western blot band shown in Figure S1A; Figure S7: Entire Western blot membranes which correspond to the cropped Western blot band shown in Figure S1B.

Author Contributions: S.I.M. and A.C.R. conceptualised and designed this study. S.I.M. and L.F. performed most of the research and analysis. P.C. participated in cell culture and transfection. S.I.M. wrote the paper with critical edits from A.C.R. with the agreement of the others. All authors have read and agreed to the published version of this manuscript.

Funding: This work was financed by the European Regional Development Fund (ERDF) through Centro 2020 Regional Operational Programme under project CENTRO-01-0145-FEDER-000012-HealthyAging2020 and through the COMPETE 2020—Operational Programme for Competitiveness and Internationalisation and Portuguese national funds via FCT—Fundação para a Ciência e a Tecnologia, under projects UIDB/04539/2020, UIDP/04539/2020 and LA/P/0058/2020. SM was supported by FCT post-doctoral fellowship SFRH/BPD/99219/2013 and is supported by FCT (Ref: DL57/2016/CP1448/CT0027). LF was supported by the FCT fellowship (SFRH/BD/148263/2019).

Institutional Review Board Statement: All animal experiments were carried out in accordance with the guidelines of the Institutional Animal Care and Use of Committee and the European Community directive (2010/63/EU) and protocols approved by the Faculty of Medicine, University of Coimbra (ref: ORBEA_211_2018) and the Direção Geral de Alimentação e Veterinária (DGAV, ref: 0421/000/000/2019). All efforts were made to minimise animal suffering and to reduce the number of animals used.

Informed Consent Statement: Not applicable.

Data Availability Statement: Data and materials described in the present manuscript will be available upon adequate request.

Conflicts of Interest: The authors declare no competing financial interests or any conflicts of interest.

References

1. Roda, A.; Serra-Mir, G.; Montoliu-Gaya, L.; Tiessler, L.; Villegas, S. Amyloid-Beta Peptide and Tau Protein Crosstalk in Alzheimer's Disease. *Neural. Regen. Res.* **2022**, *17*, 1666. [\[CrossRef\]](#)
2. Younes, L.; Albert, M.; Moghekar, A.; Soldan, A.; Pettigrew, C.; Miller, M.I. Identifying Changepoints in Biomarkers During the Preclinical Phase of Alzheimer's Disease. *Front. Aging Neurosci.* **2019**, *11*, 74. [\[CrossRef\]](#)
3. Fortin, D.A.; Srivastava, T.; Soderling, T.R. Structural Modulation of Dendritic Spines during Synaptic Plasticity. *Neuroscientist* **2012**, *18*, 326–341. [\[CrossRef\]](#)
4. Godoy, J.A.; Rios, J.A.; Picón-Pagès, P.; Herrera-Fernández, V.; Swaby, B.; Crepin, G.; Vicente, R.; Fernández-Fernández, J.M.; Muñoz, F.J. Mitostasis, Calcium and Free Radicals in Health, Aging and Neurodegeneration. *Biomolecules* **2021**, *11*, 1012. [\[CrossRef\]](#)
5. Seager, R.; Lee, L.; Henley, J.M.; Wilkinson, K.A. Mechanisms and Roles of Mitochondrial Localisation and Dynamics in Neuronal Function. *Neuronal Signal.* **2020**, *4*, NS20200008. [\[CrossRef\]](#)
6. Ferreira, I.L.; Ferreira, E.; Schmidt, J.; Cardoso, J.M.; Pereira, C.M.F.; Carvalho, A.L.; Oliveira, C.R.; Rego, A.C. A β and NMDAR Activation Cause Mitochondrial Dysfunction Involving ER Calcium Release. *Neurobiol. Aging* **2015**, *36*, 680–692. [\[CrossRef\]](#)
7. Manczak, M.; Reddy, P.H. Abnormal Interaction of VDAC1 with Amyloid Beta and Phosphorylated Tau Causes Mitochondrial Dysfunction in Alzheimer's Disease. *Hum. Mol. Genet.* **2012**, *21*, 5131–5146. [\[CrossRef\]](#)
8. Kandimalla, R.; Manczak, M.; Pradeepkiran, J.A.; Morton, H.; Reddy, P.H. A Partial Reduction of Drp1 Improves Cognitive Behavior and Enhances Mitophagy, Autophagy and Dendritic Spines in a Transgenic Tau Mouse Model of Alzheimer Disease. *Hum. Mol. Genet.* **2022**, *31*, 1788–1805. [\[CrossRef\]](#)
9. Hernandez-Zimbron, L.F.; Luna-Muñoz, J.; Mena, R.; Vazquez-Ramirez, R.; Kubli-Garfias, C.; Cribbs, D.H.; Manoutcharian, K.; Gevorkian, G. Amyloid- β Peptide Binds to Cytochrome C Oxidase Subunit 1. *PLoS ONE* **2012**, *7*, e42344. [\[CrossRef\]](#)
10. Ortiz, M.A.; Mikhailova, T.; Li, X.; Porter, B.A.; Bah, A.; Kotula, L. Src Family Kinases, Adaptor Proteins and the Actin Cytoskeleton in Epithelial-to-Mesenchymal Transition. *Cell Commun. Signal.* **2021**, *19*, 67. [\[CrossRef\]](#)
11. Marotta, G.; Basagni, F.; Rosini, M.; Minarini, A. Role of Fyn Kinase Inhibitors in Switching Neuroinflammatory Pathways. *Curr. Med. Chem.* **2022**, *29*, 4738–4755. [\[CrossRef\]](#)
12. Shao, W.; Liu, L.; Zheng, F.; Ma, Y.; Zhang, J. The Potent Role of Src Kinase-Regulating Glucose Metabolism in Cancer. *Biochem. Pharmacol.* **2022**, *206*, 115333. [\[CrossRef\]](#)
13. Rajani, V.; Sengar, A.S.; Salter, M.W. Src and Fyn Regulation of NMDA Receptors in Health and Disease. *Neuropharmacology* **2021**, *193*, 108615. [\[CrossRef\]](#)
14. Dustin, C.M.; Heppner, D.E.; Lin, M.C.J.; Van Der Vliet, A. Redox Regulation of Tyrosine Kinase Signalling: More than Meets the Eye. *J. Biochem.* **2020**, *167*, 151–163. [\[CrossRef\]](#)
15. Espada, J.; Martín-Pérez, J. An Update on Src Family of Nonreceptor Tyrosine Kinases Biology. *Int. Rev. Cell Mol. Biol.* **2017**, *331*, 83–122. [\[CrossRef\]](#)
16. Roskoski, R. Src Protein-Tyrosine Kinase Structure, Mechanism, and Small Molecule Inhibitors. *Pharmacol. Res.* **2015**, *94*, 9–25. [\[CrossRef\]](#)
17. Goebel-Goody, S.M.; Davies, K.D.; Alvestad Linger, R.M.; Freund, R.K.; Browning, M.D. Phospho-Regulation of Synaptic and Extrasynaptic N-Methyl-d-Aspartate Receptors in Adult Hippocampal Slices. *Neuroscience* **2009**, *158*, 1446–1459. [\[CrossRef\]](#)
18. Salvi, M.; Brunati, A.M.; Bordin, L.; La Rocca, N.; Clari, G.; Toninello, A. Characterization and Location of Src-Dependent Tyrosine Phosphorylation in Rat Brain Mitochondria. *Biochim. Biophys. Acta Mol. Cell Res.* **2002**, *1589*, 181–195. [\[CrossRef\]](#)
19. Ogura, M.; Yamaki, J.; Homma, M.K.; Homma, Y. Mitochondrial C-Src Regulates Cell Survival through Phosphorylation of Respiratory Chain Components. *Biochem. J.* **2012**, *447*, 281–289. [\[CrossRef\]](#)
20. Costa, R.O.; Lacor, P.N.; Ferreira, I.L.; Resende, R.; Auberson, Y.P.; Klein, W.L.; Oliveira, C.R.; Rego, A.C.; Pereira, C.M.F. Endoplasmic Reticulum Stress Occurs Downstream of GluN2B Subunit of N-Methyl-d-Aspartate Receptor in Mature Hippocampal Cultures Treated with Amyloid- β Oligomers. *Aging Cell* **2012**, *11*, 823–833. [\[CrossRef\]](#)
21. Ferreira, I.L.; Bajouco, L.M.; Mota, S.I.; Auberson, Y.P.; Oliveira, C.R.; Rego, A.C. Amyloid Beta Peptide 1-42 Disturbs Intracellular Calcium Homeostasis through Activation of GluN2B-Containing N-Methyl-d-Aspartate Receptors in Cortical Cultures. *Cell Calcium* **2012**, *51*, 95–106. [\[CrossRef\]](#)
22. Alberdi, E.; Sánchez-Gómez, M.V.; Cavaliere, F.; Pérez-Samartín, A.; Zugaza, J.L.; Trullas, R.; Domercq, M.; Matute, C. Amyloid Beta Oligomers Induce Ca²⁺ Dysregulation and Neuronal Death through Activation of Ionotropic Glutamate Receptors. *Cell Calcium* **2010**, *47*, 264–272. [\[CrossRef\]](#)
23. Mota, S.I.; Ferreira, I.L.; Valero, J.; Ferreira, E.; Carvalho, A.L.; Oliveira, C.R.; Rego, A.C. Impaired Src Signaling and Post-Synaptic Actin Polymerization in Alzheimer's Disease Mice Hippocampus--Linking NMDA Receptors and the Reelin Pathway. *Exp. Neurol.* **2014**, *261*, 698–709. [\[CrossRef\]](#)

24. Mota, S.I.; Pita, I.; Águas, R.; Tagorti, S.; Virmani, A.; Pereira, F.C.; Rego, A.C. Mechanistic Perspectives on Differential Mitochondrial-Based Neuroprotective Effects of Several Carnitine Forms in Alzheimer's Disease in Vitro Model. *Arch. Toxicol.* **2021**, *95*, 2769–2784. [[CrossRef](#)]
25. Boczek, E.E.; Luo, Q.; Dehling, M.; Röpke, M.; Mader, S.L.; Seidl, A.; Kaila, V.R.I.; Buchner, J. Autophosphorylation Activates C-Src Kinase through Global Structural Rearrangements. *J. Biol. Chem.* **2019**, *294*, 13186–13197. [[CrossRef](#)]
26. Hashimoto, M.; Bogdanovic, N.; Volkmann, I.; Aoki, M.; Winblad, B.; Tjernberg, L.O. Analysis of Microdissected Human Neurons by a Sensitive ELISA Reveals a Correlation between Elevated Intracellular Concentrations of Abeta42 and Alzheimer's Disease Neuropathology. *Acta Neuropathol.* **2010**, *119*, 543–554. [[CrossRef](#)]
27. Huang, H.C.; Nguyen, T.; Pickett, C.B. Phosphorylation of Nrf2 at Ser-40 by Protein Kinase C Regulates Antioxidant Response Element-Mediated Transcription. *J. Biol. Chem.* **2002**, *277*, 42769–42774. [[CrossRef](#)]
28. Pavlov, P.F.; Petersen, C.H.; Glaser, E.; Ankarcróna, M. Mitochondrial Accumulation of APP and Abeta: Significance for Alzheimer Disease Pathogenesis. *J. Cell. Mol. Med.* **2009**, *13*, 4137–4145. [[CrossRef](#)]
29. Eckert, A.; Pagani, L. Amyloid-Beta Interaction with Mitochondria. *Int. J. Alzheimer's Dis.* **2011**, *2011*, 925050. [[CrossRef](#)]
30. Gutierrez, B.A.; Limon, A. Synaptic Disruption by Soluble Oligomers in Patients with Alzheimer's and Parkinson's Disease. *Biomedicines* **2022**, *10*, 1743. [[CrossRef](#)]
31. Williamson, R.; Scales, T.; Clark, B.R.; Gibb, G.; Hugh Reynolds, C.; Kellie, S.; Bird, I.N.; Varndell, I.M.; Sheppard, P.W.; Everall, I.; et al. Rapid Tyrosine Phosphorylation of Neuronal Proteins Including Tau and Focal Adhesion Kinase in Response to Amyloid-Beta Peptide Exposure: Involvement of Src Family Protein Kinases. *J. Neurosci.* **2002**, *22*, 10–20. [[CrossRef](#)]
32. Wang, Y.; Shi, Z.; Zhang, Y.; Yan, J.; Yu, W.; Chen, L. Oligomer β -Amyloid Induces Hyperactivation of Ras to Impede NMDA Receptor-Dependent Long-Term Potentiation in Hippocampal CA1 of Mice. *Front. Pharmacol.* **2020**, *11*, 595360. [[CrossRef](#)]
33. Li, Y.L.; Liu, F.; Zhang, Y.Y.; Lin, J.; Huang, C.L.; Fu, M.; Zhou, C.; Li, C.J.; Shen, J.F. NMDAR1-Src-Pannexin1 Signal Pathway in the Trigeminal Ganglion Contributed to Orofacial Ectopic Pain Following Inferior Alveolar Nerve Transection. *Neuroscience* **2021**, *466*, 77–86. [[CrossRef](#)] [[PubMed](#)]
34. Wu, G.M.; Du, C.P.; Xu, Y. Oligomeric A β 25–35 Induces the Tyrosine Phosphorylation of PSD-95 by SrcPTKs in Rat Hippocampal CA1 Subfield. *Int. J. Neurosci.* **2021**, *133*, 888–895. [[CrossRef](#)]
35. Ba, M.; Ding, W.; Guan, L.; Lv, Y.; Kong, M. S-Nitrosylation of Src by NR2B-NNOS Signal Causes Src Activation and NR2B Tyrosine Phosphorylation in Levodopa-Induced Dyskinetic Rat Model. *Hum. Exp. Toxicol.* **2019**, *38*, 303–310. [[CrossRef](#)]
36. Plascencia-Villa, G.; Perry, G. Roles of Oxidative Stress in Synaptic Dysfunction and Neuronal Cell Death in Alzheimer's Disease. *Antioxidants* **2023**, *12*, 1628. [[CrossRef](#)]
37. Behl, C.; Davis, J.B.; Lesley, R.; Schubert, D. Hydrogen Peroxide Mediates Amyloid β Protein Toxicity. *Cell* **1994**, *77*, 817–827. [[CrossRef](#)]
38. Kontogiorgis, C.A.; Xu, Y.; Hadjipavlou-Litina, D.; Luo, Y. Coumarin Derivatives Protection against ROS Production in Cellular Models of A β Toxicities. *Free. Radic. Res.* **2009**, *41*, 1168–1180. [[CrossRef](#)]
39. Liu, J.; Wang, M. Carvedilol Protection against Endogenous A β -Induced Neurotoxicity in N2a Cells. *Cell Stress Chaperones* **2018**, *23*, 695–702. [[CrossRef](#)] [[PubMed](#)]
40. Chen, W.B.; Wang, Y.X.; Wang, H.G.; An, D.; Sun, D.; Li, P.; Zhang, T.; Lu, W.G.; Liu, Y.Q. Role of TPEN in Amyloid-B25-35-Induced Neuronal Damage Correlating with Recovery of Intracellular Zn²⁺ and Intracellular Ca²⁺ Overloading. *Mol. Neurobiol.* **2023**, *60*, 4232–4245. [[CrossRef](#)]
41. Zhang, J.; Li, K.; Wang, X.; Smith, A.M.; Ning, B.; Liu, Z.; Liu, C.; Ross, C.A.; Smith, W.W. Curcumin Reduced H₂O₂- and G2385R-LRRK2-Induced Neurodegeneration. *Front. Aging Neurosci.* **2021**, *13*, 754956. [[CrossRef](#)]
42. Fão, L.; Coelho, P.; Duarte, L.; Vilaça, R.; Hayden, M.R.; Mota, S.I.; Rego, A.C. Restoration of C-Src/Fyn Proteins Rescues Mitochondrial Dysfunction in Huntington's Disease. *Antioxid. Redox Signal.* **2023**, *38*, 95–114. [[CrossRef](#)]
43. Swerdlow, R.H. The Alzheimer's Disease Mitochondrial Cascade Hypothesis: A Current Overview. *J. Alzheimer's Dis.* **2023**, *92*, 1–18. [[CrossRef](#)] [[PubMed](#)]
44. Zaninello, M.; Fišar, Z. Linking the Amyloid, Tau, and Mitochondrial Hypotheses of Alzheimer's Disease and Identifying Promising Drug Targets. *Biomolecules* **2022**, *12*, 1676. [[CrossRef](#)]
45. Reddy, A.P.; Yin, X.; Sawant, N.; Reddy, P.H. Protective Effects of Antidepressant Citalopram against Abnormal APP Processing and Amyloid Beta-Induced Mitochondrial Dynamics, Biogenesis, Mitophagy and Synaptic Toxicities in Alzheimer's Disease. *Hum. Mol. Genet.* **2021**, *30*, 847–864. [[CrossRef](#)]
46. Salman, M.; Akram, M.; Shahrukh, M.; Ishrat, T.; Parvez, S. Effects of Pramipexole on Beta-Amyloid1–42 Memory Deficits and Evaluation of Oxidative Stress and Mitochondrial Function Markers in the Hippocampus of Wistar Rat. *Neurotoxicology* **2022**, *92*, 91–101. [[CrossRef](#)] [[PubMed](#)]
47. Calkins, M.J.; Manczak, M.; Mao, P.; Shirendeb, U.; Reddy, P.H. Impaired Mitochondrial Biogenesis, Defective Axonal Transport of Mitochondria, Abnormal Mitochondrial Dynamics and Synaptic Degeneration in a Mouse Model of Alzheimer's Disease. *Hum. Mol. Genet.* **2011**, *20*, 4515–4529. [[CrossRef](#)] [[PubMed](#)]
48. Marinho, D.; Ferreira, I.L.; Lorenzoni, R.; Cardoso, S.M.; Santana, I.; Rego, A.C. Reduction of Class I Histone Deacetylases Ameliorates ER-Mitochondria Cross-Talk in Alzheimer's Disease. *Aging Cell* **2023**, *22*, e13895. [[CrossRef](#)] [[PubMed](#)]
49. Nygaard, H.B.; Van Dyck, C.H.; Strittmatter, S.M. Fyn Kinase Inhibition as a Novel Therapy for Alzheimer's Disease. *Alzheimer's Res. Ther.* **2014**, *6*, 8. [[CrossRef](#)] [[PubMed](#)]

50. Nygaard, H.B.; Wagner, A.F.; Bowen, G.S.; Good, S.P.; MacAvoy, M.G.; Strittmatter, K.A.; Kaufman, A.C.; Rosenberg, B.J.; Sekine-Konno, T.; Varma, P.; et al. A Phase Ib Multiple Ascending Dose Study of the Safety, Tolerability, and Central Nervous System Availability of AZD0530 (Saracatinib) in Alzheimer's Disease. *Alzheimer's Res. Ther.* **2015**, *7*, 35. [[CrossRef](#)]
51. Kaufman, A.C.; Salazar, S.V.; Haas, L.T.; Yang, J.; Kostylev, M.A.; Jeng, A.T.; Robinson, S.A.; Gunther, E.C.; Van Dyck, C.H.; Nygaard, H.B.; et al. Fyn Inhibition Rescues Established Memory and Synapse Loss in Alzheimer Mice. *Ann. Neurol.* **2015**, *77*, 953–971. [[CrossRef](#)] [[PubMed](#)]
52. Van Dyck, C.H.; Nygaard, H.B.; Chen, K.; Donohue, M.C.; Raman, R.; Rissman, R.A.; Brewer, J.B.; Koeppe, R.A.; Chow, T.W.; Rafii, M.S.; et al. Effect of AZD0530 on Cerebral Metabolic Decline in Alzheimer Disease: A Randomized Clinical Trial. *JAMA Neurol.* **2019**, *76*, 1219–1229. [[CrossRef](#)] [[PubMed](#)]

Disclaimer/Publisher's Note: The statements, opinions and data contained in all publications are solely those of the individual author(s) and contributor(s) and not of MDPI and/or the editor(s). MDPI and/or the editor(s) disclaim responsibility for any injury to people or property resulting from any ideas, methods, instructions or products referred to in the content.